HHS Public Access

Author manuscript

Mol Psychiatry. Author manuscript; available in PMC 2021 September 17.

Published in final edited form as:

Mol Psychiatry. 2021 June ; 26(6): 2483–2492. doi:10.1038/s41380-020-00993-z.

Bioenergetics and Abnormal Functional Connectivity in Psychotic Disorders

Xiaopeng Song, Ph.D.[1,2,3,7], **Xi Chen, Ph.D.**[1,2,3,7], **Cagri Yuksel, M.D.**[1,3], **Junliang Yuan, M.D.**[2,4], **Diego A. Pizzagalli, Ph.D.**[2,3,5], **Brent Forester, M.D., M.Sc.**[3,6], **Dost Öngür, M.D., Ph.D.**[1,2,3], **Fei Du, Ph.D.**[1,2,3,*]

[1]Psychotic Disorders Division, McLean Hospital, 02478, USA

[2]McLean Imaging Center, McLean Hospital, 02478, USA

[3]Harvard Medical School, Boston, Massachusetts, 02115, USA

[4]National Clinical Research Center for Mental Disorders, Peking University Sixth Hospital, Beijing 100191, China

[5]Center for Depression, Anxiety and Stress Research, McLean Hospital, 02478, USA

[6]Division of Geriatric Psychiatry, McLean Hospital, 02478, USA

[7]These authors contributed equally to this work

Abstract

Psychotic Disorders such as schizophrenia (SZ) and bipolar disorder (BD) are characterized by abnormal functional connectivity (FC) within neural networks such as the default mode network (DMN), as well as attenuated anticorrelation between DMN and task-positive networks (TPN). Bioenergetic processes are critical for synaptic connectivity and are also abnormal in psychotic disorders. We therefore examined the association between brain energy metabolism and FC in psychotic disorders. ^{31}P magnetization transfer spectroscopy from medial prefrontal cortex (MPFC) and whole-brain fMRI data were collected from demographically matched groups of SZ, BD, and healthy control (HC) subjects. The creatine kinase (CK) reaction flux calculated from spectroscopy was used as an index of regional energy production rate. FC maps were generated with MPFC as the seed region. Compared to HC, SZ showed significantly lower CK flux, while both BD and SZ patients showed decreased anticorrelation between MPFC and TPN. CK flux was significantly correlated with FC between MPFC and other DMN nodes in HC. This positive correlation was reduced modestly in BD and strongly in SZ. CK flux was negatively correlated with the anticorrelation between MPFC and TPN in HC, but this relationship was not observed in BD or SZ. These results indicate that MPFC energy metabolism rates are associated with stronger FC within networks and stronger anticorrelation between networks in HC. However, this association is decreased in SZ and BD, where bioenergetic and FC abnormalities are evident. This

[*]**Correspondence to:** Fei Du, McLean Imaging Center, McLean Hospital, Harvard Medical School, Belmont, Massachusetts, USA, 02478, fdu@mclean.harvard.edu.

Supplementary information is available at MP's website.

pattern may suggest that impairment in energy production in psychotic disorders underlies the impaired neural connectivity.

INTRODUCTION

Schizophrenia (SZ) and bipolar I disorder with psychotic features (BD) are often conceptualized as “dysconnection syndromes” characterized by abnormal within-network connectivity and between-network anticorrelation [1, 2]. The default mode network (DMN), including the medial prefrontal cortex (MPFC), posterior cingulate cortex (PCC), and bilateral inferior parietal lobule (IPL), has been implicated in these disorders characterized by impaired perception, delusions, thought disorder, abnormal emotion regulation, altered motor function, and impaired drive [1]. Functional connectivity (FC) refers to the relationship of neural activities between spatially distinct brain regions and is usually measured during resting-state fMRI. FC can be analyzed based on the temporal similarities of time series of Blood-Oxygen-Level-Dependent (BOLD) signal in anatomically distinct brain regions. A positive FC value indicates co-activation of these regions, while a negative FC value shows anticorrelation in which one region is activated while the other is deactivated. Although there are some discrepancies in the literature, most studies report abnormal FC within DMN and reduced anticorrelation between DMN and task positive networks (TPN) in both BD and SZ patients [3].

Other lines of evidence have implicated bioenergetics and mitochondrial dysfunction in BD and SZ [4–6]. Adenosine triphosphate (ATP) is the brain’s primary energy source. Although ATP is generated de novo by oxidative phosphorylation in mitochondria, its HEP moiety is rapidly transferred to creatine to generate phosphocreatine (PCr) in a reaction catalyzed by the reversible enzyme creatine kinase (CK). PCr diffuses throughout the cytosol and is used to regenerate ATP locally via the CK reaction as required for cellular reactions. Therefore, PCr acts as a HEP reservoir and maintains stable ATP levels despite changes in neuronal activity; the CK reaction is the main source of ATP generation in the cytosol. The flow of metabolites through the CK reaction (abbreviated CK flux) can be quantified in vivo using a technique called ^{31}P magnetization transfer magnetic resonance spectroscopy (^{31}P-MT-MRS) [4, 5].

Although much progress has been made in the evaluation of bioenergetic and FC changes in psychotic disorders [4–6], no study has directly assessed whether regional energy metabolism is related to FC in SZ or BD. Sustaining normal brain circuit function places a large energy demand on the brain, but we do not have direct evidence for any relationship between bioenergetic dysfunction and abnormal connectivity. Here, we used ^{31}P-MT-MRS to determine CK flux in MPFC, and BOLD-fMRI to measure resting-state FC using a MPFC seed. Since energy metabolism and related mitochondrial functions are critical for sustaining fundamental neuronal mechanisms (including maintenance of ion gradients, intracellular signaling, and synaptic neurotransmission) and BOLD signal is correlated with local field potential and synaptic activity [7], we hypothesized that FC would be associated with regional bioenergetic activity indicated by CK flux, and this relationship would be abnormal in

psychotic disorders. To control for potential confounding from white matter abnormalities, we also examined white matter integrity using diffusion tensor imaging (DTI).

MATERIALS AND METHODS

Subjects

Participants were 27 SZ patients, 39 BD I patients with psychotic features, and 29 healthy controls (HCs). This study was approved by the McLean Hospital Institutional Review Board. All participants provided written informed consent. Patients were recruited from McLean Hospital (Belmont, MA). Diagnostic assessments were carried out using the Structured Clinical Interview for DSM-IV for patients and HCs. The Positive and Negative Syndrome Scale (PANSS), the Young Mania Rating Scale (YMRS), the Montgomery-Åsberg Depression Rating Scale (MADRS), and the Multnomah Community Ability Scale (MCAS) scores were collected. Sociodemographic and clinical characteristics of participants are presented in Table 1. Except for 10 patients (5 BD and 5 SZ), all patients were using psychiatric medications at the time of the scan (see Supplementary Table 1). No patients had significant past or current neurological or medical disorders, intellectual disability, or history of head trauma with loss of consciousness; or had received electroconvulsive therapy within the previous year. We also excluded individuals using supplements such as creatine that affect high-energy phosphate (HEP) levels. The HC group met the same criteria and in addition had no personal or first-degree relative history of any psychotic disorders. We had previously reported data from ten of the patients in the BD group [5].

Magnetic Resonance Imaging

All participants underwent brain structural and functional imaging on a 3.0-Tesla MRI scanner (Siemens Tim-Trio, Erlangen, Germany), as well as MRS on a 4.1-Tesla scanner. All subjects were at awake and eyes-open (without fixation) condition. Foam pads were used to minimize head motion during scanning. High-resolution T1-weighted images, BOLD-fMRI, and diffusion tensor imaging (DTI) data were acquired for each subject (see Supplementary materials).

In Vivo ^{31}P-MT-MRS Experiments

The ^{31}P-MT-MRS data were collected using a 4.0-Tesla whole-body imaging system (Unity/Inova; Varian NMR Instruments, California, USA) with a specially designed half-helmet surface coil with dual tuned proton and phosphorus frequency channels placed on the forehead. The MRS voxel was positioned on the frontal lobe and localized shimming was performed. The ^{31}P-MT pulse sequence and experimental design have been described previously (see Supplementary materials, and Supplementary Figure 1) [4, 6, 8, 9].

fMRI Data Processing

Prior to FC analysis, fMRI data were preprocessed using SPM12 (http://www.fil.ion.ucl.ac.uk/spm) software (see Supplementary materials). For FC analysis, a spherical region of 10 mm radius located in the MPFC (MNI coordinate, [0, 44, 31]) was selected as the seed region. FC between regional mean time series for the MPFC seed region and all other voxels was calculated with a canonical correlation approach. Individual FC

maps were converted into z-scored maps with Fisher's-z transformation and subjected to second-level, random-effects analysis to generate group-level statistical maps.

Since global signal regression may enhance anti-correlation between DMN and TPN[10, 11], we performed the same fMRI analyses with/without regressing out the global signal. We also quantified the amplitude of global signal and tested its correlation with CK flux.

In addition to FC, we also quantified local neural activity using additional approaches: Regional Homogeneity (ReHo) [12, 13], Amplitude of Low Frequency Fluctuation (ALFF) [14], and fractional ALFF (fALFF) [14, 15]. Please see Supplementary materials for details.

DTI Data Processing

The diffusion tensor was computed at each voxel, the resultant eigenvalues were used to compute the fractional anisotropy (FA) [16]. Whole-brain tract-based spatial statistics (TBSS) was performed for multi-subject analysis of FA (see Supplementary materials).

^{31}P-MRS Data Processing

The data processing was performed using FID-A [17]. The detailed calculation of chemical exchange reaction among PCr and ATP as well as the relative chemical reaction parameters, which has been described in our previous publications [4–6, 9, 18], are described in the Supplementary materials.

Statistical Analyses

All data processing of above was blinded to diagnosis before statistical analyses. Demographic and clinical data were examined using Chi-square (categorical values) and independent samples t-tests (numerical values). Our primary outcome measures were CK flux (F) and FC. We tested group differences in CK flux using an ANCOVA with diagnosis as a between-subjects factor and with age, sex, and medication dose (see Supplementary materials) as covariates.

We performed two-sided one-sample t-tests on the FC maps of patients and controls combined, to examine brain areas that were significantly correlated or anticorrelated with the MPFC [covariates, age and sex; False discovery rate (FDR) corrections for multiple comparisons, $p<0.05$]. We compared the FC maps between SZ and controls, BD vs. controls, and SZ vs. BD subjects respectively using analysis of covariance (ANCOVA; covariates, age and sex; FDR, $p<0.05$).

We further examined cross-subject partial correlations between the FC maps and CK flux in each group. Since the fMRI and MRS data were collected from different scanners on different dates, the difference of days apart between the scans of the two modalities (15.5±16.9 days) was included as a covariate in addition to age, sex, and medication (FDR corrections for multiple comparisons, corrected $p<0.05$). The average FC values within the DMN and TPN areas derived from one-sample t-tests were extracted for each participant, and their cross-subjects correlation with CK flux was calculated for each group. ANCOVA was used to test whether the correlation between CK flux and FC was significantly different

among the three groups. The same correlation analyses with CK flux were performed for the local brain activity measurements (ReHo, ALFF, fALFF) in MPFC as secondary analyses.

For DTI data, the skeletonized FA maps were fed into a group-level analysis in FSL. Family wise error (FWE) was calculated using the non-parametric permutation test with 5000 permutations. Different white matter regions of interest (ROIs) are defined according to the Johns Hopkins University white matter atlas [19]. The average FA values within these ROIs were extracted from the individual skeletons and included as covariates in a second correlation analysis between CK flux and FC.

RESULTS

Demographic and clinical variables

There were no statistically significant differences in age or sex between groups (Table 1). Among the clinical measures, some expected differences were observed; e.g. SZ patients had significantly higher PANSS negative scores than BD patients, and both SZ and BD patients showed lower MCAS scores compared to HC. All the data in the manuscript were expressed as mean± standard deviation.

CK flux

CK Flux was statistically significantly lower in SZ (45.7±11.1 mol/g/min) compared to HC (52.2±10.9 mol/g/min) ($F_{1,52}$=5.59, p=0.022, η_p^2=0.10) and BD (50.9±10.6 mol/g/min) ($F_{1,62}$=4.27, p=0.043, η_p^2=0.064), but not significantly different between HC and BD ($F_{1,64}$=0.69, p=0.41, η_p^2=0.011). The variances of CK flux were similar between SZ and HC ($F_{26,28}$=0.91, p=1.04), BD and HC ($F_{38,28}$=0.95, p=0.86), SZ and BD ($F_{26,38}$=0.76, p=1.11).

Functional Connectivity

In healthy controls, MPFC showed significant positive FC with the canonical DMN areas, including PCC, bilateral angular gyrus, lateral orbital frontal cortices, and inferior temporal cortices, and significant negative correlation with TPN areas, including bilateral superior parietal lobule (SPL), supra marginal gyrus, dorsal lateral prefrontal cortices, supplementary motor areas (SMA), superior temporal gyrus, insula, lingual gyrus, and middle occipital gyrus (Figure 1A, see Supplementary Figure 2 for whole-brain t-map without thresholding).

Compared to HC, both BD and SZ groups showed significant decreased anticorrelation between MPFC and bilateral SPL (Figures 1B and C, respectively). The SZ group showed a further reduction in the anticorrelation between MPFC and SPL when compared to the BD group (Figure 1D). Whole-brain t-maps without thresholding are shown in Supplementary Figure 3–5.

Correlation between CK flux and FC

For clarity, we present positive and negative correlation results separately in Figure 2. Higher CK flux was positively correlated with FC between MPFC and PCC, and bilateral angular gyrus in HC. The pattern of correlation was weaker in BD, where it was only seen

between MPFC and PCC/right angular gyrus, and even weaker in SZ where it was found only between MPFC and PCC (Figure 2A).

Higher CK flux was associated with stronger negative FC between MPFC and multiple TPN areas in HC, including SPL, supramarginal gyrus, SMA, insula, lingual gyrus, and middle occipital gyrus. This association pattern between CK flux and negative FC was weaker in BD and SZ groups. In BD, CK flux was correlated with negative FC between MPFC and SPL/left middle occipital gyrus; in SZ CK flux was correlated with negative FC between MPFC and SPL/lingual gyrus (Figure 2B). Whole-brain r-maps without thresholding are shown in Supplementary Figure 6–8.

We next used an ROI analysis to better understand the relationships between CK flux and MPFC connectivity at the network level. Among HC, CK flux was significantly correlated with positive FC between MPFC and other nodes of DMN ($r=0.72$, $p<0.001$). This positive correlation was reduced but still significant in BD ($r=0.47$, $p=0.0032$), and further diminished in SZ ($r=0.34$, $p=0.079$) (Figure 3A). ANCOVA showed that the correlation coefficients between CK flux and within-DMN FC were significantly different among the three groups (covariates: age and sex, $F_{2,87}=6.13$, $p=0.0032$, $\eta_p^2=0.12$). Post-hoc analysis showed this correlation was significantly higher in HC than in SZ ($F_{1,50}=13.28$, $p<0.001$, $\eta_p^2=0.21$). CK flux was also statistically significantly correlated with the negative FC between MPFC and TPN in HC ($r=-0.68$, $p<0.001$), but not in BD ($r=-0.088$, $p=0.60$) or SZ ($r=-0.19$, $p=0.35$) (Figure 3B). ANCOVA showed that the correlations between CK flux and MPFC-TPN FC were significantly different among the three groups ($F_{2,87}=11.55$, $p<0.001$, $\eta_p^2=0.21$). Post-hoc analysis showed this correlation was significantly stronger in HC than in SZ ($F_{1,50}=13.29$, $p<0.001$, $\eta_p^2=0.21$) and BD ($F_{1,62}=16.6$, $p<0.001$, $\eta_p^2=0.21$); and for an alpha level of 0.05, our sample achieved 97.6% and 97.5% power (1-beta) to detect differences in the FC-CK flux correlations between SZ and HC, as well as BD and HC respectively.

It is notable that the above results did not change significantly when the global signal of fMRI was not regressed out (Supplementary Figure 9). There is no significant group difference in global signal amplitude between SZ and HC ($t=0.86$, $p=0.40$), BD and HC ($t=0.97$, $p=0.33$), or SZ and BD ($t=-0.10$, $p=0.92$) in our sample. Therefore, we performed correlation analyses between CK flux and the amplitude of global signal across all the subjects ($n=95$) and found that this correlation was not statistically significant ($r=-0.16$, $p=0.11$).

Correlation of flux with local activity

There was a significant positive correlation between CK flux and ReHo in the ventral MPFC (but not ALFF and fALFF) within the HC group. No significant correlations were observed for any of the MPFC local activity measurements in BD or SZ (Supplementary Figure 10).

DTI

TBSS showed no statistically significant difference in FA between any of the three groups (Supplementary Figure 11). Furthermore, including the mean FA values within different

white matter templates (Supplementary table 2) as covariates did not change the results of correlation analysis between flux and FC in all of three group subjects.

DISCUSSION

In the current study, we report significant abnormalities in brain bioenergetics, brain circuit connectivity, as well as a breakdown in the relationship between these two processes in SZ and BD. The bioenergetic and connectivity findings have been previously reported [2, 4, 5]. However, the analysis of the relationship between the two here provides novel insights into the neurobiology of psychotic disorders. We also recognize a pattern where reported abnormalities are typically less pronounced in BD than in SZ when compared with HC, despite the fact that our BD group includes only patients with bipolar I disorder with psychotic features, i.e. patients more similar to SZ in presentation and outcome than those with other subtypes of BD. Our findings are even more striking because we found no evidence for impaired white matter integrity in our patient samples. In other words, the FC abnormalities exist in the absence of a commensurate breakdown in white matter microstructure.

Reduced CK flux in SZ is consistent with our previous studies in chronic SZ [4] and first episode BD with psychotic features [5], suggesting that this is a common feature across psychotic disorders. It is also consistent with post-mortem studies highlighting reduced CK activity and immunoreactivity [20] and reduced CK brain isoenzyme content [21] in SZ. Moreover, mitochondrial CK activity is tightly coupled to oxidative phosphorylation [22], and the activity of both CK isoforms are reduced by oxidative damage [23]. Therefore, lower CK flux reflects an abnormal bioenergetic state in psychotic disorders which is characterized by impaired mitochondrial energy production, lower brain metabolic rate, and increased oxidative stress [24].

It was not surprising that we detected decreased anticorrelation between the DMN and the TPN in the BD and SZ patients. Multiple studies have found these significantly reduced anticorrelations in psychotic patients [2, 3, 25, 26]. Evidence from experiments with healthy subjects using resting-state and task-based fMRI suggested that the anticorrelation between the DMN and TPN are important for distinguishing or switching between external stimuli or task and self-referential thoughts [15]. In line with these studies, our results suggest that the loss of a TPN-DMN anticorrelation may reflect insufficient segregation of internally and externally focused states and disturbance of cognition in psychotic disorders [26].

The anti-correlation between DMN and TPN may be associated with the global signal of the resting-state fMRI [11, 27]. Our results showed global signal regression did enhance anticorrelation in this study. However, the difference of FC between patients and HC, as well as the correlations between FC and CK flux did not change significantly before and after global signal regression, indicating that the impaired functional segregation between DMN and TPN is an intrinsic feature of psychotic disorders. Moreover, converging evidence suggests a link between the global signal and brain vigilance level, i.e. lower vigilance states, such as light sleep stage [28], hypnotic drugs usage [29, 30], are characterized by a larger amplitude of global signal fluctuation; while elevated vigilance levels are associated with a

weaker global signal component[31]. It has been reported that schizophrenia patients show a stronger global resting-state fMRI component than healthy controls[32]. In our data sample, there was no significant between-group difference in the amplitude of global signal. Indeed, we found a trend of negative correlation between CK flux and the amplitude of global signal across all the subjects. This is in line with previous reports and may indicate that higher brain energy metabolism is associated with higher vigilance level.

Given the role of PCr/CK system in maintaining ATP, reduced CK flux in psychotic disorders indicates a susceptibility for failing to meet energy requirements. Failure to produce or utilize energy can impair energy-dependent brain functions, such as synaptic activity and depolarization of axons, ultimately leading to reduced ability to synchronize neuronal activity across remote sites resulting in abnormal FC. In addition, energy metabolism and mitochondrial activity are closely linked to other critical mechanisms, including redox imbalance and signaling, neuroinflammation and calcium ion homeostasis. These factors may further affect neural activity and lead to impaired FC in SZ and BD [33, 34].

We observed a strong association between MPFC regional CK flux and FC in this study. Although this correlation was decreased in the SZ and BD, the flux was still significantly correlated with the FC between MPFC and PCC, as well as the anticorrelation between MPFC and parts of the TPN. These results suggest that the faster the energy metabolism the stronger the functional integration/segregation within circuits, especially for long-distance and large-scale neuronal communications. Previous studies found that CK flux is correlated with brain activity levels, i.e. reduced when activity is limited during anesthesia [9] and increased with brain activation [35]. Studies combining positron emission tomography and MRI also reported that higher glucose metabolism was associated with higher degree of functional centrality [36]. Together with these studies, our results indicate that the tight association between bioenergetic metabolism and FC might be a general principle of brain energy-activity organization.

On the other hand, the breakdown of the relationship between CK flux and FC in psychotic disorders is striking. Here, using in vivo ^{31}P-MT-MRS, we found a reduction in the activity of a critical enzyme involved in brain energy metabolism (CK) and a breakdown of the normal relationship between CK flux and FC. Since greater CK flux is associated with greater positive FC within and greater negative FC between networks in the healthy brain, it is not surprising that respective impairments in bioenergetics and FC are associated with a breakdown of the normal relationship. The parallel findings in our ReHo analysis further indicate that both remote and local neural synchronization are regulated by regional energy metabolism. Situated between the SZ and controls, BD showed a moderate correlation between CK flux and FC. We also note that the breakdown between CK flux and FC in psychotic disorders was most pronounced for anticorrelations. This may indicate that functional segregation between brain networks is more energetically costly than functional integration within a network.

What are the potential explanations for loss of metabolism-neural activity coupling in psychotic disorders? One is a limited capability to utilize the regional PCr reservoir to maintain local and remote neural synchronization, and thus a higher demand of glycolysis

or other oxidative phosphorylation processes. Another is that brain cells may need more energy for maintaining basic "housekeeping" functions in psychotic patients, siphoning resources away from functional coupling mechanisms. In general, most of the ATP energy budget (40–60%) in the brain is spent for neuronal synapses, maintaining and restoring the transmembrane Na^+/K^+ ion gradients that are diminished by neuronal firing associated with spontaneous brain activity [37]. The rest of ATP is used for "housekeeping" functions that maintain basic cellular integrity in the brain, such as phospholipid metabolism, DNA transcription, and proteins synthesis. Thus, brain "housekeeping" activities and spontaneous neural activity each use approximately half of the total brain ATP [9]. It is possible that "housekeeping" activity consumes more energy in SZ and BD, resulting in less energy available for building up local or remote neural synchronization.

Although there's substantial evidence of abnormalities in white matter in BD and SZ [38], our current findings cannot be explained by white matter abnormalities. In previous work, some studies report reduced FA in SZ and BD in frontal and temporal regions [39, 40], whereas others do not [41–43], and some even find increased structural connectivity in psychotic spectrum patients [44]. Explanations for these inconsistent results include the large variability in DTI data acquisition, processing and analysis protocols, and the heterogeneity of subject populations [45]. In the current study, we did not find any statistically significant difference in DTI between HC, BD, and SZ. In addition, including the mean FA values as covariate did not significantly change the correlation between CK flux and FC. Taken together, this suggests that the FC abnormalities in our data cannot be explained by white matter abnormalities but instead are associated with bioenergetic processes.

Several limitations should be mentioned. First, the spatial resolution of ^{31}P-MT-MRS is limited due to the low intrinsic detection sensitivity. The methodological limitations of traditional ^{31}P-MT-MRS approaches [46] as currently implemented necessitate long scanning times required for acquiring reliable data. This results in poor spatial resolution, as evidenced in the fact that our MRS measurement signal came from a large frontal region. There have been efforts to develop more efficient methods [6]. We have suggested a novel ^{31}P-MT-approach-T_1^{nom} aimed at rapidly mapping energy-ATP metabolic fluxes [47]. This approach has been used to map CK/ATPase activity in the human brain with 3D spatial mapping [48] but is technically challenging and has not been implemented in clinical studies. Therefore, the current work is a foundation for future studies at 7T where shorter scans are possible. Second, our DTI data were of relatively low quality. To shorten experiment time, we used 6-direction diffusion gradients. This precludes any high-resolution fiber tracking and illustration of fiber projections from MPFC to correlated nodes. However, FA should be accurate enough with 6-direction diffusion gradients, and this would not change our observation that we find no significant changes when FA was added to the model. Third, our MRI and ^{31}P-MRS data were collected during different experimental sessions because we optimized data collection with fMRI at 3T and MRS at 4T. Although the number of days between scans was regressed out as a covariate, it may introduce spurious sources of variance into our analyses. Finally, there is the issue of heterogeneity of patient populations, a common challenge in clinical research. We included all available unmedicated or medicated patients, including chronic and first episode patients. Since some subjects were taking multiple medications, it is difficult to study the exact link between FC/CK flux and a

specific type of drug, considering the limited sample sizes. Nevertheless, we used ANOVA to test the association between FC/CK flux and the medications usage in all the patients, the results (Supplementary Table 3) showed no significant relationship between any specific type of medication and FC/CK flux. Moreover, including the medication information as covariates in the correlation analyses did not change the relationship between FC and CK flux. We note that our patient groups are in their mid-20s, indicating that on average they can be characterized as “early phase”. This mitigates, although does not exclude, any potential effects of disease duration and taking medications on MRI/MRS measures.

In conclusion, by combining in vivo ^{31}P-MT-MRS and fMRI, we report significant correlations between MPFC energy metabolic rate and its FC with long-distance and large-scale brain networks and a breakdown of this relationship in psychotic disorders. The tight association between bioenergetics and FC might be a general principle of brain energy-activity organization and reduced flux through the CK reaction may disrupt FC in SZ and BD. Further research is needed to develop treatment approaches targeting this metabolism-neural synchrony pathway.

Supplementary Material

Refer to Web version on PubMed Central for supplementary material.

ACKNOWLEDGMENTS

The authors thank our volunteers and Mr. Elliot Kuan, and Ms. Margaret Gardner for their assistance in the experiments and subject recruitment. This research work was supported by National Institutes of Health (NIH) grants: R21MH114020, R01MH114982, P50MH115846, K24MH104449, R01AG066670.

CONFLICT OF INTEREST

Over the past 3 years, Dr. Pizzagalli has received consulting fees from Akili Interactive Labs, BlackThorn Therapeutics, Boehringer Ingelheim, Compass Pathway, Otsuka Pharmaceuticals, and Takeda Pharmaceuticals; one honorarium from Alkermes, and research funding from NIMH, Dana Foundation, Brain and Behavior Research Foundation, Millennium Pharmaceuticals. In addition, he has received stock options from BlackThorn Therapeutics. Dr. Forester has received research funding from the NIA, Rogers Family Foundation, Spier Family Foundation, Eli Lilly and Biogen and consulting fees from Biogen. Dr. Yuksel received research support from Diamentis Inc. No funding from these entities was used to support the current work, and all views expressed are solely those of the authors. None of the other authors have conflict of interest to declare.

REFERENCES

1. Friston K, Brown HR, Siemerkus J, Stephan KE. The dysconnection hypothesis (2016). Schizophrenia research2016; 176(2–3): 83–94. [PubMed: 27450778]
2. Whitfield-Gabrieli S, Thermenos HW, Milanovic S, Tsuang MT, Faraone SV, McCarley RWet al.Hyperactivity and hyperconnectivity of the default network in schizophrenia and in first-degree relatives of persons with schizophrenia. Proceedings of the National Academy of Sciences2009; 106(4): 1279–1284.
3. Hu ML, Zong XF, Mann JJ, Zheng JJ, Liao YH, Li ZCet al.A Review of the Functional and Anatomical Default Mode Network in Schizophrenia. Neuroscience bulletin2017; 33(1): 73–84. [PubMed: 27995564]
4. Du F, Cooper AJ, Thida T, Sehovic S, Lukas SE, Cohen BMet al.In Vivo Evidence for Cerebral Bioenergetic Abnormalities in Schizophrenia Measured Using 31P Magnetization Transfer SpectroscopySchizophrenia Cerebral Bioenergetic AbnormalitiesSchizophrenia Cerebral Bioenergetic Abnormalities. JAMA Psychiatry2014; 71(1): 19–27. [PubMed: 24196348]

5. Du F, Yuksel C, Chouinard VA, Huynh P, Ryan K, Cohen BMet al.Abnormalities in High-Energy Phosphate Metabolism in First-Episode Bipolar Disorder Measured Using (31)P-Magnetic Resonance Spectroscopy. Biological psychiatry2018; 84(11): 797–802. [PubMed: 28527566]
6. Du F, Zhu XH, Qiao H, Zhang X, Chen W. Efficient in vivo 31P magnetization transfer approach for noninvasively determining multiple kinetic parameters and metabolic fluxes of ATP metabolism in the human brain. Magnetic resonance in medicine2007; 57(1): 103–114. [PubMed: 17191226]
7. Logothetis NK. The underpinnings of the BOLD functional magnetic resonance imaging signal. Journal of Neuroscience2003; 23(10): 3963–3971. [PubMed: 12764080]
8. de Graaf RA, Luo Y, Garwood M, Nicolay K. B1-Insensitive, Single-Shot Localization and Water Suppression. Journal of Magnetic Resonance, Series B1996; 113(1): 35–45. [PubMed: 8888589]
9. Du F, Zhu XH, Zhang Y, Friedman M, Zhang N, Ugurbil Ket al.Tightly coupled brain activity and cerebral ATP metabolic rate. Proceedings of the National Academy of Sciences of the United States of America2008; 105(17): 6409–6414. [PubMed: 18443293]
10. Murphy K, Fox MD. Towards a consensus regarding global signal regression for resting state functional connectivity MRI. NeuroImage2017; 154: 169–173. [PubMed: 27888059]
11. Liu TT, Nalci A, Falahpour M. The global signal in fMRI: Nuisance or Information? NeuroImage2017; 150: 213–229. [PubMed: 28213118]
12. Song X, Zhang Y, Liu Y. Frequency specificity of regional homogeneity in the resting-state human brain. PloS one2014; 9(1).
13. Zang Y, Jiang T, Lu Y, He Y, Tian L. Regional homogeneity approach to fMRI data analysis. NeuroImage2004; 22(1): 394–400. [PubMed: 15110032]
14. Zou Q-H, Zhu C-Z, Yang Y, Zuo X-N, Long X-Y, Cao Q-Jet al.An improved approach to detection of amplitude of low-frequency fluctuation (ALFF) for resting-state fMRI: fractional ALFF. Journal of neuroscience methods2008; 172(1): 137–141. [PubMed: 18501969]
15. Song X, Qian S, Liu K, Zhou S, Zhu H, Zou Qet al.Resting-state BOLD oscillation frequency predicts vigilance task performance at both normal and high environmental temperatures. Brain structure & function2017; 222(9): 4065–4077. [PubMed: 28600679]
16. Basser PJ, Mattiello J, LeBihan D. Estimation of the effective self-diffusion tensor from the NMR spin echo. Journal of magnetic resonance Series B1994; 103(3): 247–254. [PubMed: 8019776]
17. Simpson R, Devenyi GA, Jezzard P, Hennessy TJ, Near J. Advanced processing and simulation of MRS data using the FID appliance (FID-A)-An open source, MATLAB-based toolkit. Magnetic resonance in medicine2017; 77(1): 23–33. [PubMed: 26715192]
18. Hetherington HP, Spencer DD, Vaughan JT, Pan JW. Quantitative (31)P spectroscopic imaging of human brain at 4 Tesla: assessment of gray and white matter differences of phosphocreatine and ATP. Magnetic resonance in medicine2001; 45(1): 46–52. [PubMed: 11146485]
19. Mori S, Oishi K, Jiang H, Jiang L, Li X, Akhter Ket al.Stereotaxic white matter atlas based on diffusion tensor imaging in an ICBM template. NeuroImage2008; 40(2): 570–582. [PubMed: 18255316]
20. Burbaeva G, Savushkina OK, Boksha IS. Creatine kinase BB in brain in schizophrenia. World J Biol Psychiatry2003; 4(4): 177–183. [PubMed: 14608589]
21. Klushnik TP, Spunde A, Yakovlev AG, Khuchua ZA, Saks VA, Vartanyan ME. Intracellular alterations of the creatine kinase isoforms in brains of schizophrenic patients. Mol Chem Neuropathol1991; 15(3): 271–280. [PubMed: 1807268]
22. Guzun R, Timohhina N, Tepp K, Monge C, Kaambre T, Sikk Pet al.Regulation of respiration controlled by mitochondrial creatine kinase in permeabilized cardiac cells in situ. Importance of system level properties. Biochim Biophys Acta2009; 1787(9): 1089–1105. [PubMed: 19362066]
23. Schlattner U, Tokarska-Schlattner M, Wallimann T. Mitochondrial creatine kinase in human health and disease. Biochim Biophys Acta2006; 1762(2): 164–180. [PubMed: 16236486]
24. Hazlett EA, Vaccaro DH, Haznedar MM, Goldstein KE. (F-18)Fluorodeoxyglucose positron emission tomography studies of the schizophrenia spectrum: The legacy of Monte S. Buchsbaum, M.D. Psychiatry Res2019; 271: 535–540.
25. Williamson PAre anticorrelated networks in the brain relevant to schizophrenia?Schizophrenia bulletin2007; 33(4): 994–1003. [PubMed: 17493957]

26. Wotruba D, Michels L, Buechler R, Metzler S, Theodoridou A, Gerstenberg Met al.Aberrant coupling within and across the default mode, task-positive, and salience network in subjects at risk for psychosis. Schizophrenia bulletin2014; 40(5): 1095–1104. [PubMed: 24243441]
27. Fox MD, Zhang D, Snyder AZ, Raichle ME. The global signal and observed anticorrelated resting state brain networks. Journal of neurophysiology2009; 101(6): 3270–3283. [PubMed: 19339462]
28. Fukunaga M, Horovitz SG, van Gelderen P, de Zwart JA, Jansma JM, Ikonomidou VNet al.Large-amplitude, spatially correlated fluctuations in BOLD fMRI signals during extended rest and early sleep stages. Magnetic resonance imaging2006; 24(8): 979–992. [PubMed: 16997067]
29. Kiviniemi VJ, Haanpää H, Kantola J-H, Jauhiainen J, Vainionpää V, Alahuhta Set al.Midazolam sedation increases fluctuation and synchrony of the resting brain BOLD signal. Magnetic resonance imaging2005; 23(4): 531–537. [PubMed: 15919598]
30. Licata SC, Nickerson LD, Lowen SB, Trksak GH, MacLean RR, Lukas SE. The hypnotic zolpidem increases the synchrony of BOLD signal fluctuations in widespread brain networks during a resting paradigm. NeuroImage2013; 70: 211–222. [PubMed: 23296183]
31. Wong CW, Olafsson V, Tal O, Liu TT. The amplitude of the resting-state fMRI global signal is related to EEG vigilance measures. NeuroImage2013; 83: 983–990. [PubMed: 23899724]
32. Yang GJ, Murray JD, Repovs G, Cole MW, Savic A, Glasser MFet al.Altered global brain signal in schizophrenia. Proceedings of the National Academy of Sciences2014; 111(20): 7438–7443.
33. Jevtic G, Nikolic T, Mircic A, Stojkovic T, Velimirovic M, Trajkovic Vet al.Mitochondrial impairment, apoptosis and autophagy in a rat brain as immediate and long-term effects of perinatal phencyclidine treatment - influence of restraint stress. Prog Neuropsychopharmacol Biol Psychiatry2016; 66: 87–96. [PubMed: 26655035]
34. Yuksel C, Du F, Ravichandran C, Goldbach JR, Thida T, Lin Pet al.Abnormal high-energy phosphate molecule metabolism during regional brain activation in patients with bipolar disorder. Molecular psychiatry2015; 20(9): 1079–1084. [PubMed: 25754079]
35. Chen W, Zhu XH, Adriany G, Ugurbil K. Increase of creatine kinase activity in the visual cortex of human brain during visual stimulation: a 31P magnetization transfer study. Magnetic resonance in medicine1997; 38(4): 551–557. [PubMed: 9324321]
36. Tomasi D, Wang GJ, Volkow ND. Energetic cost of brain functional connectivity. Proceedings of the National Academy of Sciences of the United States of America2013; 110(33): 13642–13647. [PubMed: 23898179]
37. Attwell D, Laughlin SB. An energy budget for signaling in the grey matter of the brain. Journal of cerebral blood flow and metabolism : official journal of theInternational Society of Cerebral Blood Flow and Metabolism2001; 21(10): 1133–1145.
38. Du F, Ongur D. Probing myelin and axon abnormalities separately in psychiatric disorders using MRI techniques. Frontiers in integrative neuroscience2013; 7: 24. [PubMed: 23596402]
39. Scheel M, Prokscha T, Bayerl M, Gallinat J, Montag C. Myelination deficits in schizophrenia: evidence from diffusion tensor imaging. Brain Structure and Function2013; 218(1): 151–156. [PubMed: 22327232]
40. Kumar J, Iwabuchi S, Oowise S, Balain V, Palaniyappan L, Liddle PF. Shared white-matter dysconnectivity in schizophrenia and bipolar disorder with psychosis. Psychological medicine2015; 45(4): 759–770. [PubMed: 25089761]
41. Mamah D, Ji A, Rutlin J, Shimony JS. White matter integrity in schizophrenia and bipolar disorder: Tract- and voxel-based analyses of diffusion data from the Connectom scanner. NeuroImage Clinical2019; 21: 101649. [PubMed: 30639179]
42. Boos HB, Mandl RC, van Haren NE, Cahn W, van Baal GC, Kahn RSet al.Tract-based diffusion tensor imaging in patients with schizophrenia and their non-psychotic siblings. European neuropsychopharmacology : the journal of the European College of Neuropsychopharmacology2013; 23(4): 295–304. [PubMed: 22841128]
43. Clark K, Narr KL, O'Neill J, Levitt J, Siddarth P, Phillips Oet al.White matter integrity, language, and childhood onset schizophrenia. Schizophrenia research2012; 138(2–3): 150–156. [PubMed: 22405729]
44. Bracht T, Viher PV, Stegmayer K, Strik W, Federspiel A, Wiest Ret al.Increased structural connectivity of the medial forebrain bundle in schizophrenia spectrum disorders is associated with

delusions of paranoid threat and grandiosity. NeuroImage Clinical2019; 24: 102044. [PubMed: 31678911]

45. Kubicki M, McCarley R, Westin CF, Park HJ, Maier S, Kikinis Ret al.A review of diffusion tensor imaging studies in schizophrenia. Journal of psychiatric research2007; 41(1–2): 15–30. [PubMed: 16023676]
46. Degani H, Laughlin M, Campbell S, Shulman RG. Kinetics of creatine kinase in heart: a ^{31}P NMR saturation- and inversion-transfer study. Biochemistry1985; 24(20): 5510–5516. [PubMed: 4074712]
47. Kim SY, Chen W, Ongur D, Du F. Rapid and simultaneous measurement of phosphorus metabolite pool size ratio and reaction kinetics of enzymes in vivo. J Magn Reson Imaging2018; 47(1): 210–221. [PubMed: 28480619]
48. Zhu XH, Qiao H, Du F, Xiong Q, Liu X, Zhang Xet al.Quantitative imaging of energy expenditure in human brain. NeuroImage2012; 60(4): 2107–2117. [PubMed: 22487547]

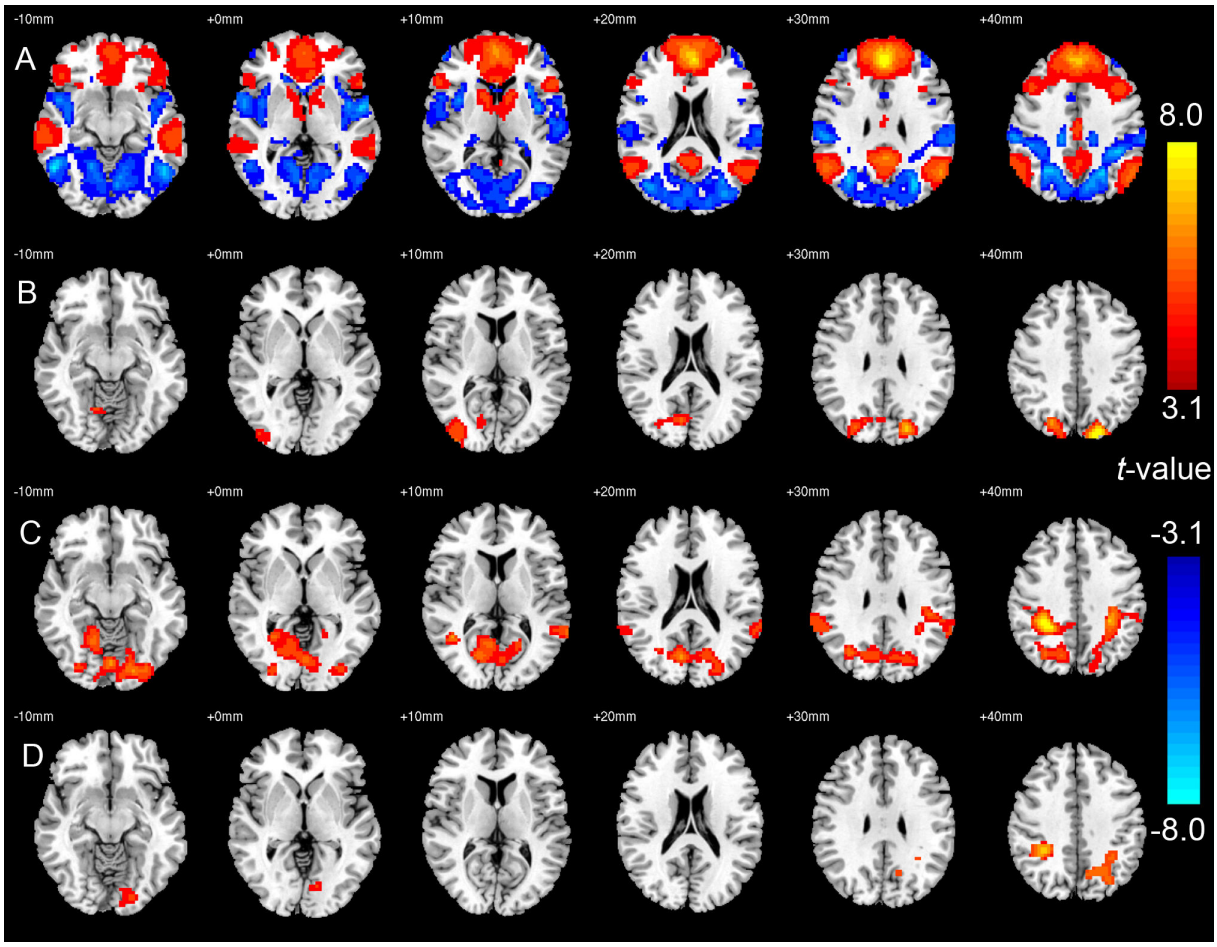

Figure 1:

(A) Default mode network and the anticorrelated task-positive network in healthy controls (HC), indicated by cold and warm colors respectively. (B) Areas with decreased anti-correlation with medial prefrontal cortex (MPFC) in bipolar disorder (BD, n=39) compared to HC (n=29). (C) Areas with decreased anti-correlation with MPFC in schizophrenia (SZ, n=27) compared to HC (n=29). (D) Areas with decreased anti-correlation with MPFC in SZ (n=27) compared to BD (n=39). In all figures, threshold was set to FDR corrected $p<0.05$. In the plot of (B) to (D), the differences were indicated by the warm colors. Images are shown in radiological convention with left side of the brain displayed on the right side of the image.

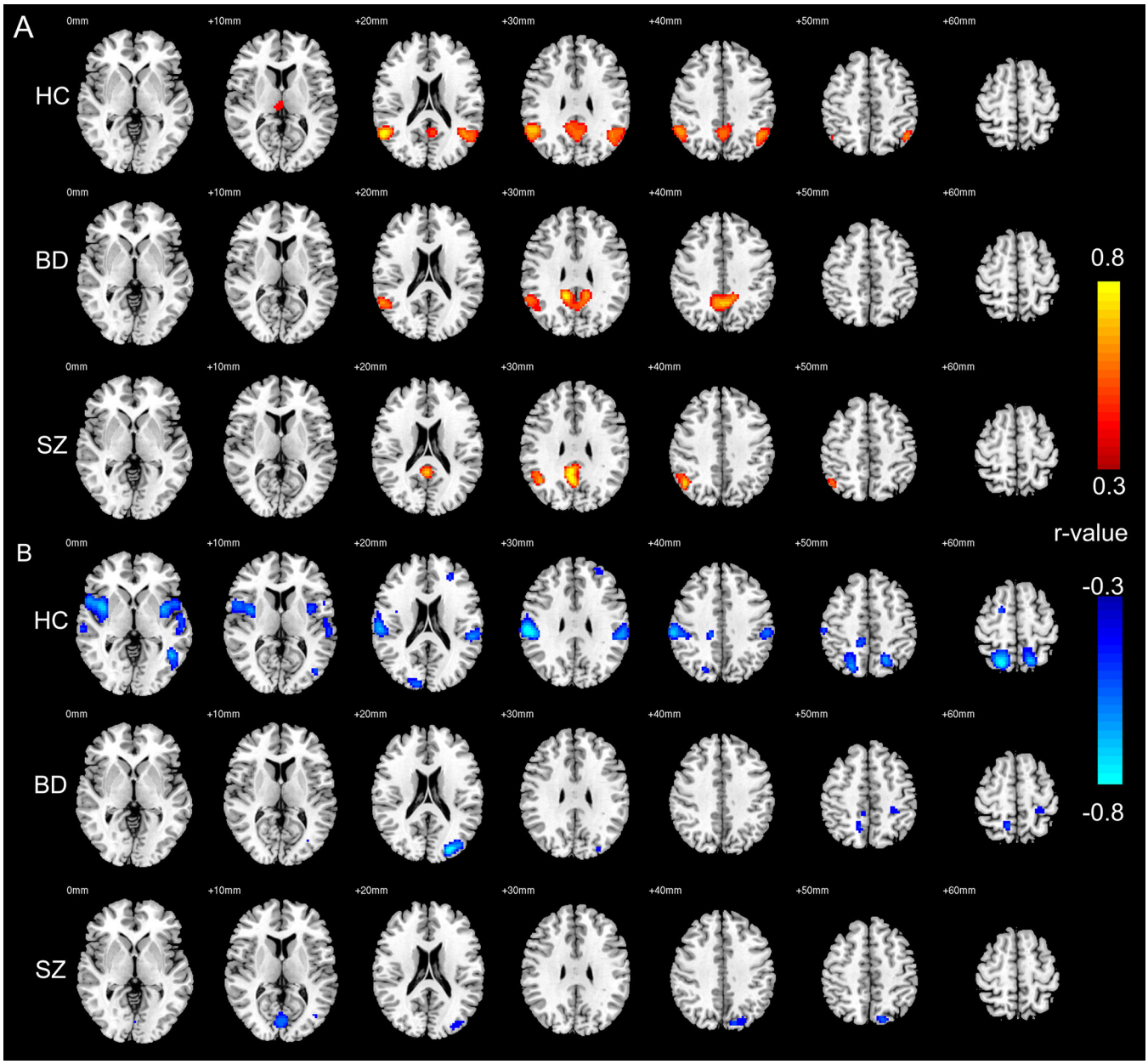

Figure 2:

(A) Brain areas whose functional connectivity (FC) with medial prefrontal cortex (MPFC) is significantly correlated with CK Flux, in healthy controls (HC, n=29), bipolar disorder (BD, n=39), and schizophrenia (SZ, n=27). (B) Brain areas whose FC with MPFC is negatively correlated with CK Flux, in HC (n=29), BD (n=39), and SZ (n=27). Images are shown in radiological convention with left side of the brain displayed on the right side of the image.

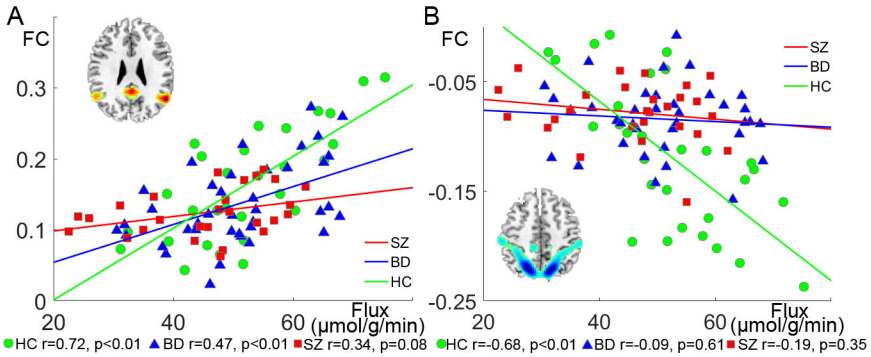

Figure 3:

(A) Correlation of CK flux and the functional connectivity (FC) between medial prefrontal cortex (MPFC) and other default mode network (DMN) areas, in healthy controls (HC, n=29, bipolar disorder (BD, n=39), and schizophrenia (SZ, n=27). (B) Correlation of CK flux and the FC between MPFC and task-positive network (TPN) areas in HC (n=29), BD (n=39), and SZ (n=27).

Table 1:

Demographic and clinical data for schizophrenia (SZ), bipolar disorder (BD), and healthy control (HC) subjects (p-values not corrected for multiple comparisons).

Variables	SZ (n = 27)	BD (n=39)	HC (n = 29)	p-values SZ vs. BD	p values SZ vs. HC	p values BP vs. HC
Mean age (years)	25.6 ± 7.5	24.2 ± 4.2	22.7 ± 3.3	0.35	0.063	0.11
Sex (Male: Female)	19:8	25:14	17:12	0.60	0.37	0.65
Disease duration (years)	4.6 ± 6.2	2.6 ± 2.4	-	0.078	-	-
PANSS General	26.3 ± 7.5	22.4 ± 6.0	-	**0.026**	-	-
PANSS Positive	12.0 ± 5.1	10.2 ± 4.7	-	0.15	-	-
PANSS Negative	12.9 ± 6.1	9.0 ± 3.1	-	**0.002**	-	-
YMRS	5.5 ± 5.0	5.4 ± 6.9	-	0.98	-	-
MADRS	8.6 ± 6.8	7.8 ± 6.7	-	0.63	-	-
MCAS	45.6 ± 6.7	48.7 ± 6.0	54.8±0.4	0.065	**<0.0001**	**0.001**

Mean ± standard deviation